

Electronic Supplementary Information

Oxygenated copper vanadium selenide composite nanostructures as a cathode material for zinc-ion batteries with high stability up to 10 000 cycles

D. Narsimulu, B. N. Vamsi Krishna, R. Shanthappa, and Jae Su Yu*

Department of Electronics and Information Convergence Engineering, Institute for Wearable Convergence Electronics, Kyung Hee University, 1732 Deogyeong-aero, Giheung-gu, Yongin-si, Gyeonggi-do 17104, Republic of Korea

*Corresponding author.

Email address: jsyu@khu.ac.kr (J. S. Yu)

1. Experimental procedure

1.1. Materials

Following chemicals, such as copper (II) nitrate trihydrate ($\text{CuH}_6\text{N}_2\text{O}_9$, Sigma Aldrich, 99%), selenious acid ($\text{Se}_2\text{H}_2\text{O}_3$, Sigma Aldrich, 99%), 2-methylimidazole ($\text{C}_4\text{H}_6\text{N}_2$, Sigma Aldrich, 99%), ammonia meta vanadate (NH_4VO_3 , Sigma Aldrich, 99%), metallic Zn (Sigma Aldrich, 0.1 cm thickness), zinc trifluoromethanesulfonate ($\text{Zn}(\text{CF}_3\text{SO}_3)_2$, Sigma Aldrich, 98%), and ZnCF (Sigma Aldrich, 98%), were utilized without further purification. The carbon fiber cloth (CFC) textile was received from the Nara Cell-Tech Corp., South Korea. Distilled water was produced in our laboratory by using a Milli-Q water equipment.

1.2. Material characterizations

The phase confirmation of the prepared samples was analyzed by X-ray diffraction (XRD; Rigaku MiniFlex 600 X-ray diffractometer with Cu K_α radiation). The morphology and fine structure of the powder sample were characterized by using a field-emission scanning electron microscope (FE-SEM; JEOL JSM-7500F) and a transmission electron microscope (TEM, JEOL- JEM). The valance states of the sample were examined by X-ray photoelectron spectroscopy (XPS; PHI 5000 VersaProbe ESCALAB 250xi).

1.3. Electrochemical measurements

The O-CuVSe cathode material slurry was prepared by mixing 70 wt% of active material, 15 wt% polyvinylidene fluoride, and 15 wt% of super P carbon in N-methyl 2 pyrrolidinone solvent. The well-mixed slurry was coated on a CFC substrate using a brush. The electrode was dried at 80 °C for 12 h in a vacuum over. After proper drying, O-CuVSe coated CFC was cut into circular discs. The mass loading of active material over the CFC substrate is around 1–2 mg cm^{-2} . The CR2032 coin-type cells were assembled in an air atmosphere using 2M ZnCF as an electrolyte, Zn metal

was employed as an anode, and GF/D glass fiber membrane (Whatman) was used as a separator. The galvanostatic charge-discharge (GCD) curves at various current densities and cyclic voltammetry (CV) curves at various scan rates were measured using the Wonna Tech battery cycler between the potential window of 0.4-2.0 V (vs. Zn/Zn²⁺).

Table S1. Comparison of the electrochemical performance of the O-CuVSe cathode material along with the previously reported cathode materials.

Cathode material	Electrolyte	Voltage (V)	Reversible capacity (mA h g^{-1})	Current density (A g^{-1})	Cycles	Ref.
Cu_{2-x}Se	2M ZnSO_4	0.4–1.6	70	5	3000	1
$\text{ZnMn}_2\text{O}_4/\text{Mn}_2\text{O}_3$	2M ZnSO_4	0.8–1.9	80	1	1000	2
ZnMn_2O_4	2M ZnSO_4 with 0.05M MnSO_4	0.8–1.9	106.5	0.1	300	3
$\text{Ni}_x\text{Mn}_{3-x}\text{O}_4$	(2M ZnSO_4 with 0.15M MnSO_4)	1.0–1.8	128.8	0.4	850	4
$\text{ZnNi}_{0.5}\text{Mn}_{0.5}\text{CoO}_4@\text{C}$	2M ZnSO_4 with 0.1M MnSO_4	1.0–1.8	110	0.2	500	5
MoS_2	3M $\text{Zn}(\text{CF}_3\text{SO}_3)_2$	0.2–1.3	125	2	500	6
$\text{MoS}_2@\text{N}$	3M $\text{Zn}(\text{CF}_3\text{SO}_3)_2$	0.2–1.3	100	1	600	7
MoO_3	1M ZnSO_4	0.2–1.9	35	1	1000	8
$\text{VS}_2@\text{N-doped carbon}$	3 M $\text{Zn}(\text{CF}_3\text{SO}_3)_2$	0.2–1.8	144	1	600	9
$\alpha\text{-MnO}_2@\text{C}$	1M ZnSO_4	1.0–1.8	189	0.066	50	10
$\text{MnO}@{\text{NGS}}$	2M ZnSO_4	0.9–1.8	112.3	0.5	300	11
$\text{Cu}_3\text{V}_2\text{O}_7(\text{OH})_2 \cdot 2\text{H}_2\text{O}$	2.5M $\text{Zn}(\text{CF}_3\text{SO}_3)_2$	0.2–1.6	100.1	0.2	130	12
CuHCF	1M ZnSO_4	1.4–2.0	44	0.1	50	13
CuHCF	1M ZnSO_4	0.8–1.9	40	0.02	20	14
CuHCF	20mM ZnSO_4	1.4–2.1	53	1	50	15
ZnHCF	1M ZnSO_4	0.8–2.0	49.4	0.06	100	16
$\text{ZnHCF}@{\text{MnO}_2}$	0.5M ZnSO_4	1.4–1.9	70	0.5	1000	17
$\text{ZnNi}_{1/2}\text{Mn}_{1/2}\text{CoO}_4$	0.3M $\text{Zn}(\text{OTf})_2$ in MeCN	0.9–2.15	174	1	200	18
Mo_6S_8	1 M ZnSO_4	0.25–1.0	87.4	0.18	150	19
$\text{CC}@\text{MnO}_2@\text{MXene}$	0.1M $\text{Mn}(\text{CH}_3\text{COO})_2$ with 0.01M Na_2SO_4	0.8–1.9	80.6	1	800	20
O-CuVSe	2M $\text{Zn}(\text{CF}_3\text{SO}_3)_2$	0.4–2.0	166.6 117	1 2 5	1000 2000 10000	This work

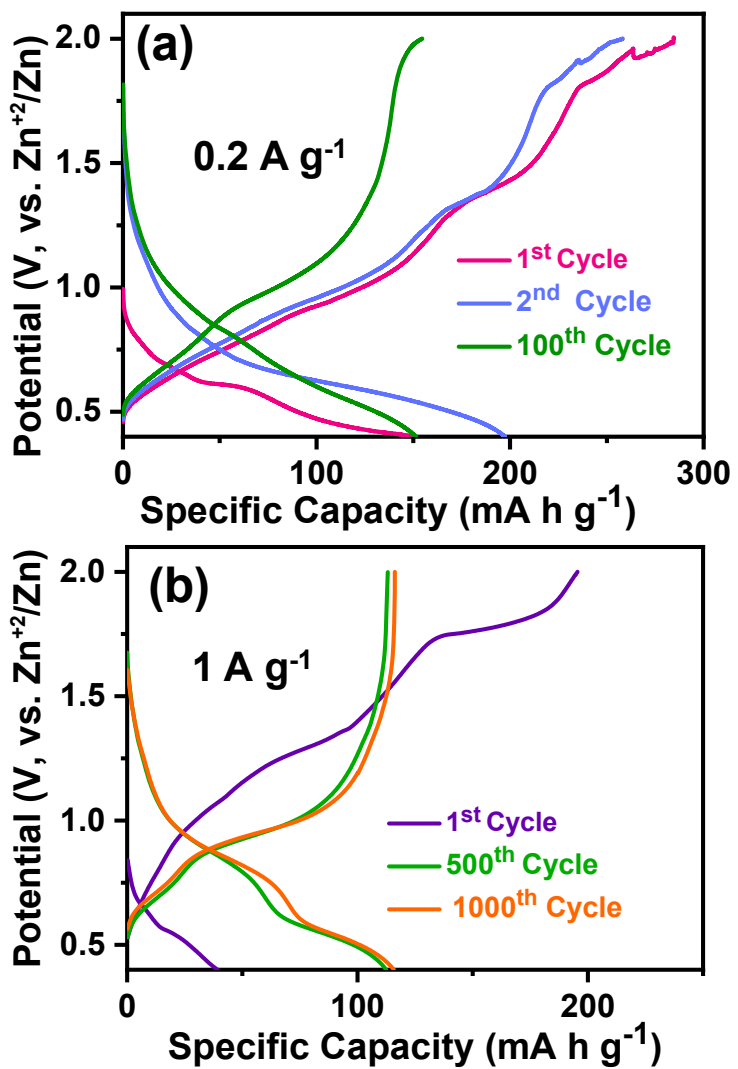


Fig. S1 Cycling performance of the O-CuVSe cathode at (a) 0.2 A g^{-1} and (b) 1 A g^{-1} .

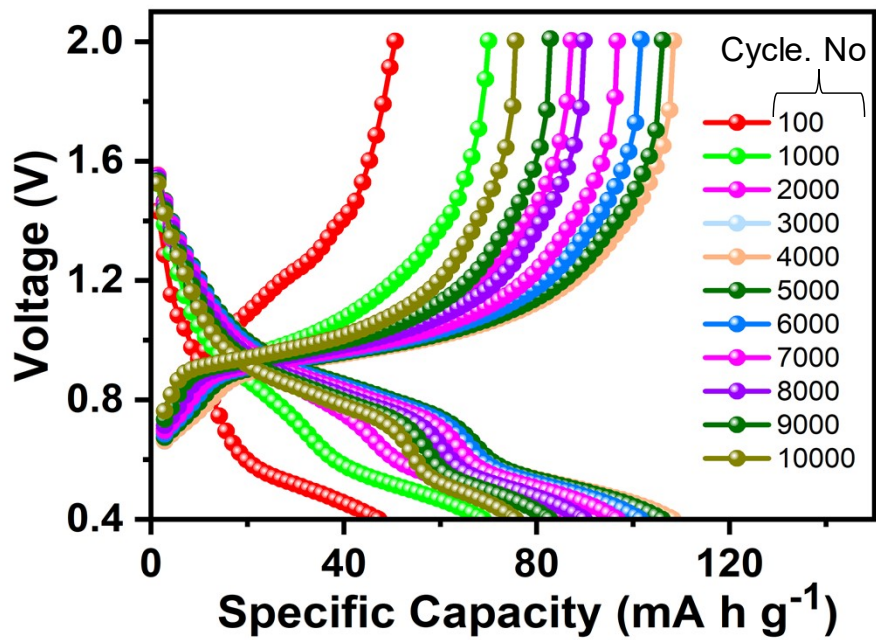


Fig. S2 Voltage profile curves of the O-CuVSe cathode at 5 A g^{-1} .

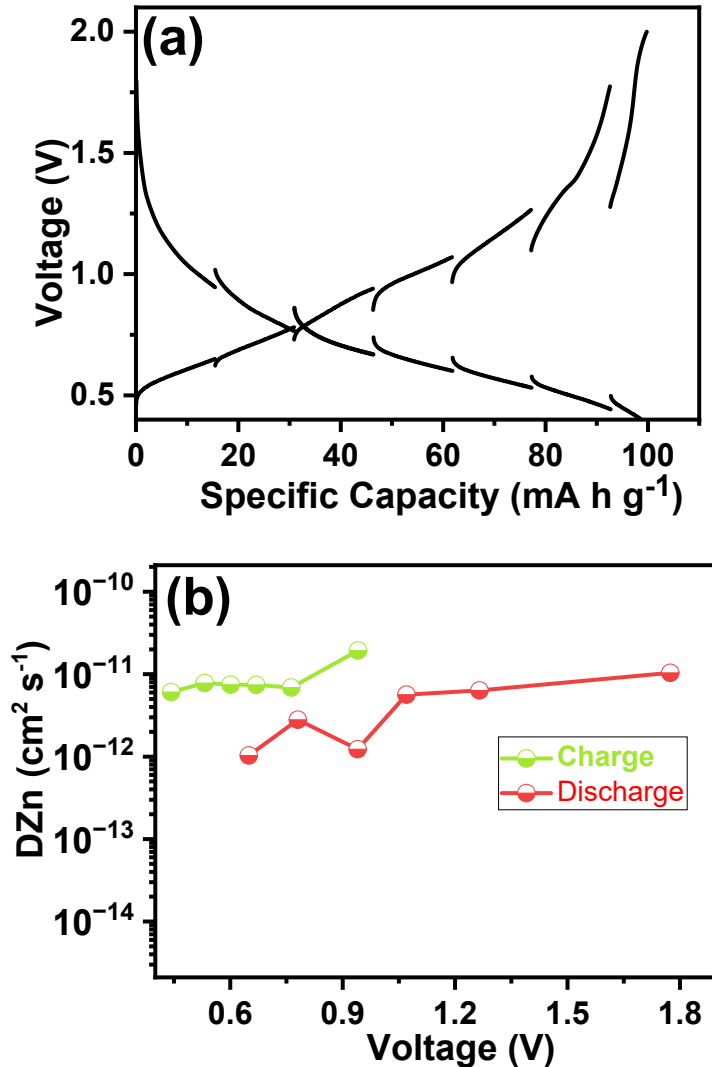


Fig. S3 (a) GITT curves and (b) corresponding diffusivity coefficient for Zn^{2+} in $\text{Zn}/\text{O-CuVSe}$ battery *vs.* voltage.

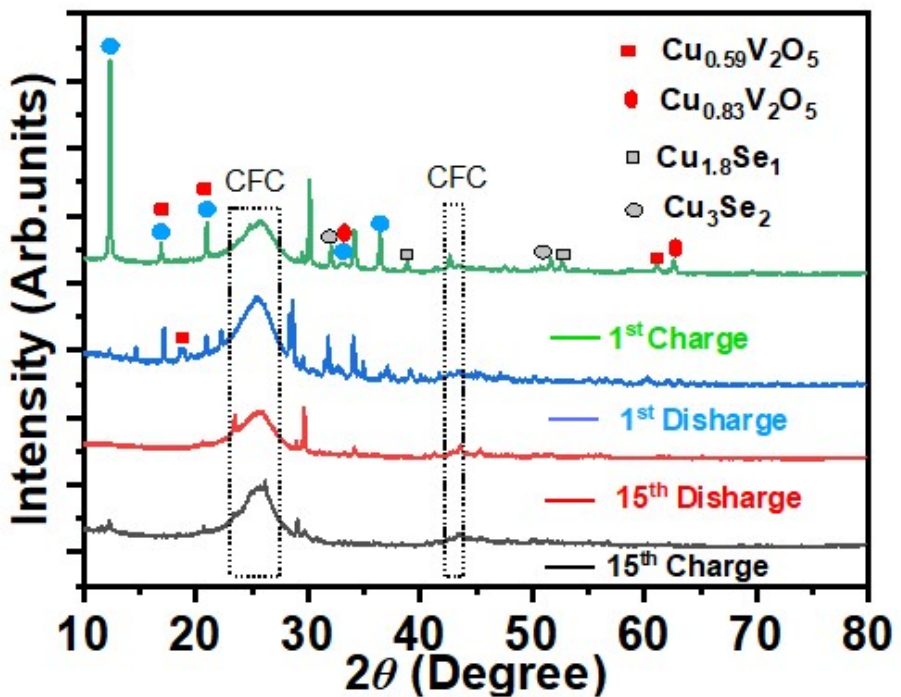


Fig. S4 Ex-situ XRD patterns of the O-CuVSe composite cathode measured after the 1st charge/discharge and 15th charge/discharge cycles.

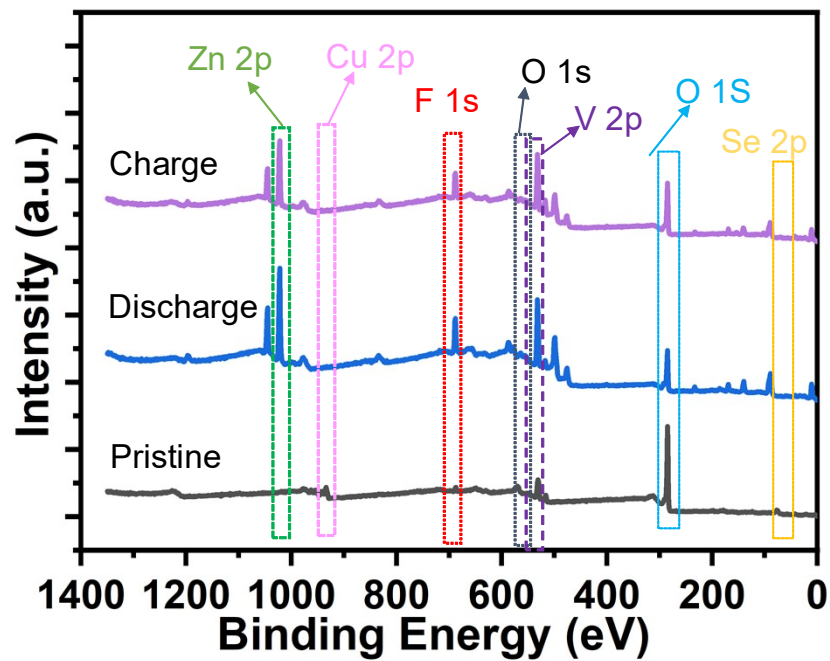


Fig. S5 XPS survey scan spectra of the O-CuVSe cathode in pristine, charge, and discharge states.

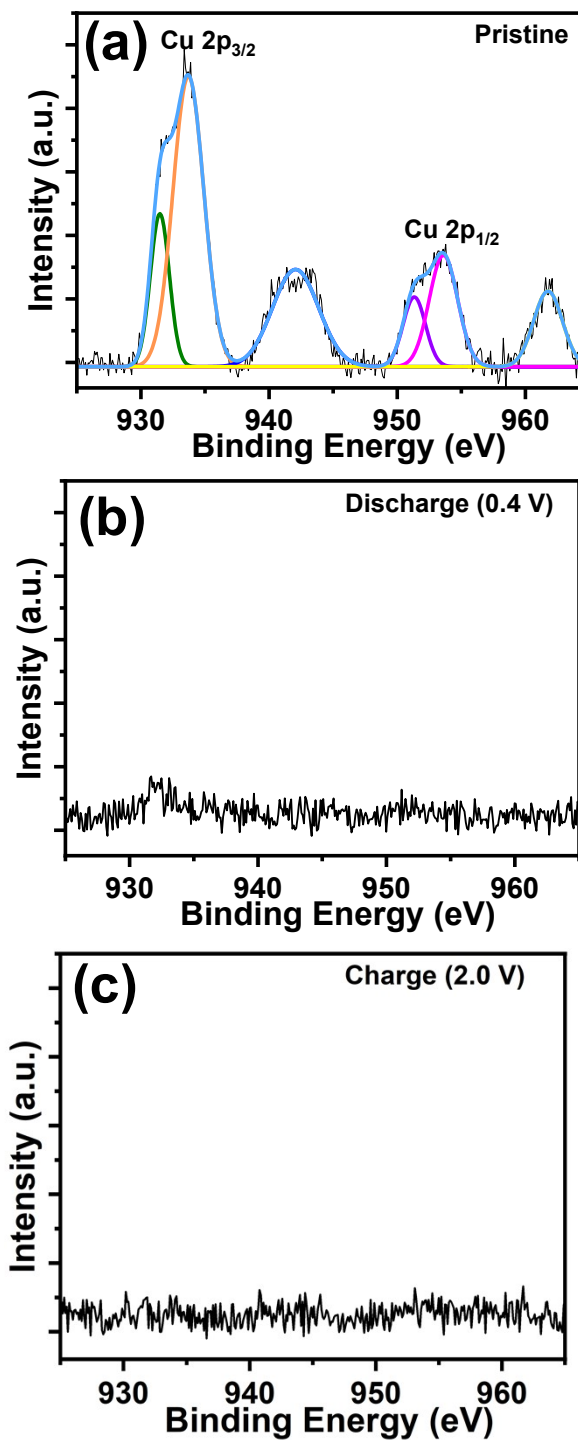


Fig. S6 High-resolution Cu 2p XPS spectra: (a) pristine state, (b) discharge state, and (c) charge state.

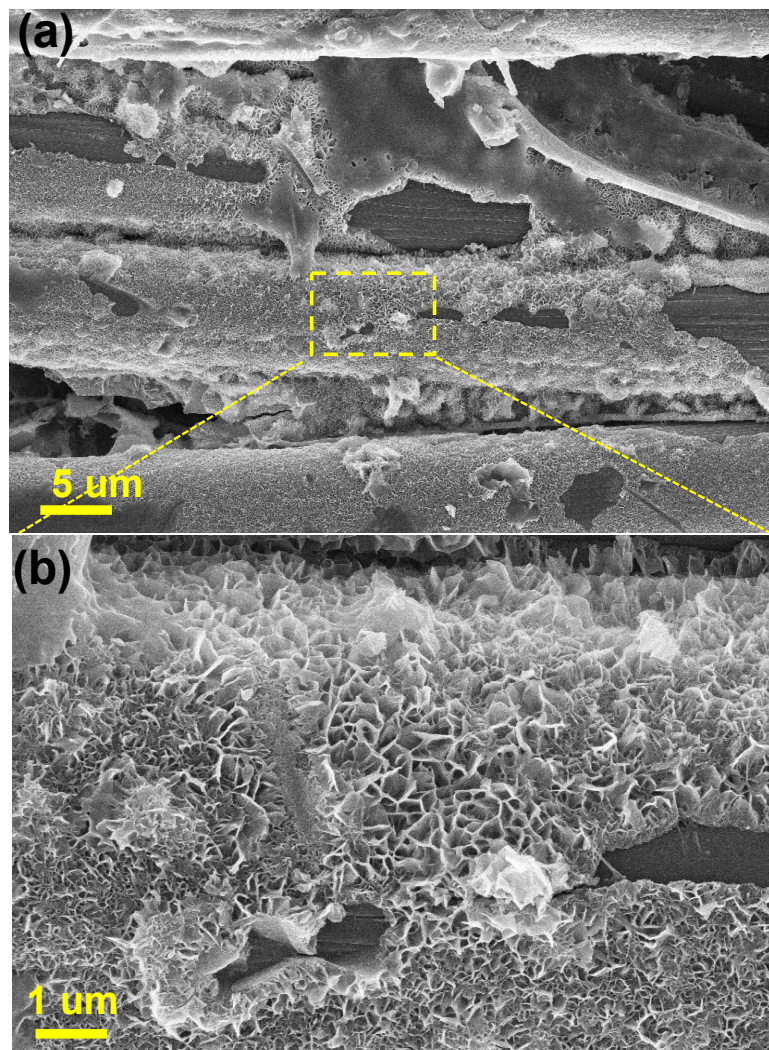


Fig. S7 (a) Low- and (b) high-magnification FE-SEM images for the O-CuVSe cathode after 2000 cycles at 2 A g^{-1} .

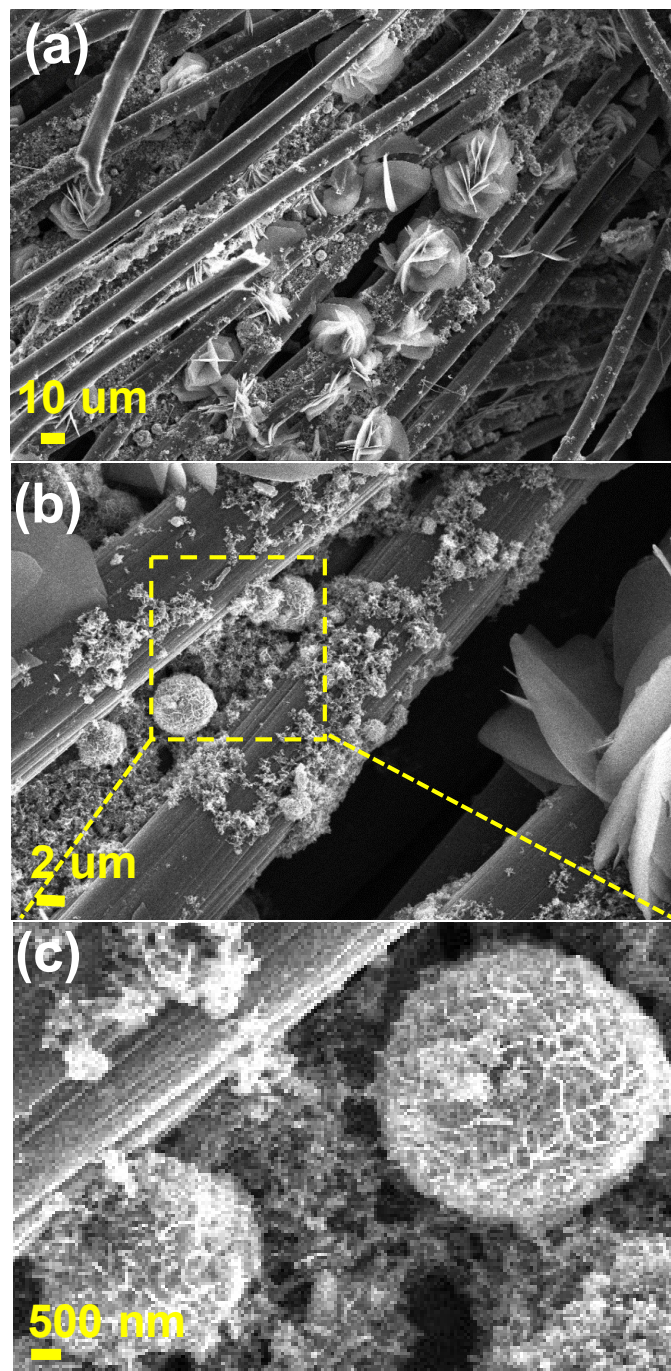


Fig. S8 (a-c) FE-SEM images under different magnifications for the O-CuVSe cathode after 10000 cycles at 5 A g^{-1} .

References

1. Y. Yang, J. Xiao, J. Cai, G. Wang, W. Du, Y. Zhang, X. Lu, and C. C. Li, *Adv. Funct. Mater.*, 2021, **31**, 2005092.
2. S.-C. Ma, M. Sun, S.-X. Wang, D.-S. Li, W.-L. Liu, M.-M. Ren, F.-G. Kong, S.-J. Wang, and Y.-M. Xia, *Scr. Mater.*, 2021, **194**, 113707.
3. X. Wu, Y. Xiang, Q. Peng, X. Wu, Y. Li, F. Tang, R. Song, Z. Liu, Z. He, and X. Wu, *J. Mater. Chem. A*, 2017, **5**, 17990-17997.
4. J. Long, J. Gu, Z. Yang, J. Mao, J. Hao, Z. Chen, and Z. Guo, *J. Mater. Chem. A*, 2019, **7**, 17854-17866.
5. F. Xing, X. Shen, Y. Chen, X. Liu, T. Chen, and Q. Xu, *Dalton Trans.*, 2021, **50**, 5795-5806.
6. C. Cai, Z. Tao, Y. Zhu, Y. Tan, A. Wang, H. Zhou, and Y. Yang, *Nanoscale Adv.*, 2021, **3**, 3780-3787.
7. Z. Sheng, P. Qi, Y. Lu, G. Liu, M. Chen, X. Gan, Y. Qin, K. Hao, and Y. Tang, *ACS Appl. Mater. Interfaces*, 2021, **13**, 34495-34506.
8. T. Xiong, Y. Zhang, Y. Wang, W. S. V. Lee, and J. Xue, *J. Mater. Chem. A*, 2020, **8**, 9006-9012.
9. J. Liu, W. Peng, Y. Li, F. Zhang, and X. Fan, *Mater. Chem. C*, 2021, **9**, 6308-6315.
10. S. Islam, M. H. Alfaruqi, J. Song, S. Kim, D. T. Pham, J. Jo, S. Kim, V. Mathew, J. P. Baboo, and Z. Xiu, *J. Energy Chem.*, 2017, **26**, 815-819.
11. W. Li, X. Gao, Z. Chen, R. Guo, G. Zou, H. Hou, W. Deng, X. Ji, and J. Zhao, *Chem. Eng. J.*, 2020, **402**, 125509.
12. L. Chen, Z. Yang, J. Wu, H. Chen, and J. Meng, *Electrochimica Acta*, 2020, **330**, 135347.

13. S. Kjeldgaard, M. Wagemaker, B. B. Iversen, and A. Bentien, *Mat. Adv.*, 2021, **2**, 2036-2044.
14. Z. Jia, B. Wang, and Y. Wang, *Mater. Chem. Phys.* 2015, **149**, 601-606.
15. R. Trócoli and F. La Mantia, *ChemSusChem*, 2015, **8**, 481-485.
16. L. Zhang, L. Chen, X. Zhou, and Z. Liu, *Adv. Energy Mater.*, 2015, **5**, 1400930.
17. K. Lu, B. Song, Y. Zhang, H. Ma, and J. Zhang, *J. Mater. Chem. A*, 2017, **5**, 23628-23633.
18. C. Pan, R. Zhang, R. G. Nuzzo, and A. A. Gewirth, *Adv. Energy Mater.*, 2018, **8**, 1800589.
19. Y. Cheng, L. Luo, L. Zhong, J. Chen, B. Li, W. Wang, S. X. Mao, C. Wang, V. L. Sprenkle, and G. Li, *ACS Appl. Mater. Interfaces*, 2016, **8**, 13673-13677.
20. M. Qi, F. Li, Z. Zhang, Q. Lai, Y. Liu, J. Gu, and L. Wang, *J. Colloid Interface Sci.*, 2022, **615**, 151-162.